Bypassing the Structural Bottleneck in the Ultrafast Melting of Electronic Order

L. X. Yang,[1,2,3,*] G. Rohde,[2] K. Hanff,[2] A. Stange,[2] R. Xiong,[4] J. Shi,[4] M. Bauer,[2] and K. Rossnagel[2,5,†]

[1]State Key Laboratory of Low Dimensional Quantum Physics, Department of Physics, Tsinghua University, Beijing 100084, People's Republic of China

[2]Institut für Experimentelle und Angewandte Physik, Christian-Albrechts-Universität zu Kiel, 24098 Kiel, Germany

[3]Frontier Science Center for Quantum Information, Beijing 100084, People's Republic of China

[4]Department of Physics, Wuhan University, Wuhan 430072, People's Republic of China

[5]Ruprecht-Haensel-Labor, Deutsches Elektronen-Synchrotron DESY, 22607 Hamburg, Germany

(Received 29 June 2020; accepted 23 November 2020; published 30 December 2020)

Impulsive optical excitation generally results in a complex nonequilibrium electron and lattice dynamics that involves multiple processes on distinct timescales, and a common conception is that for times shorter than about 100 fs the gap in the electronic spectrum is not seriously affected by lattice vibrations. Here, however, by directly monitoring the photoinduced collapse of the spectral gap in a canonical charge-density-wave material, the blue bronze $Rb_{0.3}MoO_3$, we find that ultrafast (∼60 fs) vibrational disordering due to efficient hot-electron energy dissipation quenches the gap significantly faster than the typical structural bottleneck time corresponding to one half-cycle oscillation (∼315 fs) of the coherent charge-density-wave amplitude mode. This result not only demonstrates the importance of incoherent lattice motion in the photoinduced quenching of electronic order, but also resolves the perennial debate about the nature of the spectral gap in a coupled electron-lattice system.

DOI: 10.1103/PhysRevLett.125.266402

In quantum materials, the coupling between the electronic and lattice degrees of freedom is often strong so that changes in the electronic properties can lead to structural distortions and vice versa. Charge-density-wave (CDW) bearing materials provide classic examples of such intertwining [1,2], as well as of the resulting controversies as to whether the transition to a charge- and lattice-modulated state and the emerging energy gap [Fig. 1(a)] are predominantly due to electron-phonon coupling or electron-electron interactions [3–6]. One allure of femtosecond time-resolved pump-probe techniques is that they can provide novel insights into this problem via temporal discrimination of electronically and lattice-driven processes [7–29]. Specifically, after impulsive photoexcitation, the electronic and lattice components of CDW order and of the energy gap can be expected to decouple because of significantly different response times. A common scenario is a multistep quench of the CDW state in which the electronic order is suppressed in less than 100 fs, while the lattice distortion is coherently relaxed on CDW amplitude-mode vibrational timescales of a few 100 fs, and incoherent lattice disordering takes place on a 1 ps timescale through electron-phonon thermalization [11–17,20,23]. *Coherent* lattice motion can thus be understood as a speed-limiting structural bottleneck for the quenching of combined charge and lattice order [8,11–14,21,27,29], although a fully *incoherent* structural transition pathway on the timescale of a single phonon oscillation is also possible [30].

In this Letter, using time- and angle-resolved photoemission spectroscopy (trARPES) [8,10,13,15], we present direct spectroscopic evidence that *incoherent* lattice motion can indeed cause complete CDW gap quenching well before *coherent* lattice motion effectively modulates the gap. Our key observation is that the initial gap quenching correlates with a surprisingly fast hot-electron energy relaxation implying a quasi-instantaneous generation of high-frequency lattice fluctuations. These photoinduced nonthermal fluctuations can rapidly fill in the gap and smear the gap edge similar to the effects of thermal lattice fluctuations [31–33] [Fig. 1(b)].

Figure 1(c) shows a schematic sketch of the trARPES experiment (details are given in the Supplemental Material) [34,35]. The technique provides a direct momentum-resolved view on energy-gap dynamics with an effective time resolution of a few 10 fs, short enough to reveal and separate the responses of the electronic and lattice components of the order [10,13,14,21]. The material is the quasi-one-dimensional blue bronze $Rb_{0.3}MoO_3$ [40], in which double chains of MoO_6 octahedra run along the crystallographic b direction [Fig. 1(c)]. This prototype CDW system undergoes a transition at $T_{CDW} \approx 180$ K, and the saturation value of the energy gap ($2\Delta_0$) is about 120 meV [5].

Figure 1(d) shows a representative ARPES band map measured without optical excitation below T_{CDW} along the one-dimensional chain (Γ-Y) direction. Consistent with high-resolution ARPES data [5,6] and the results of band

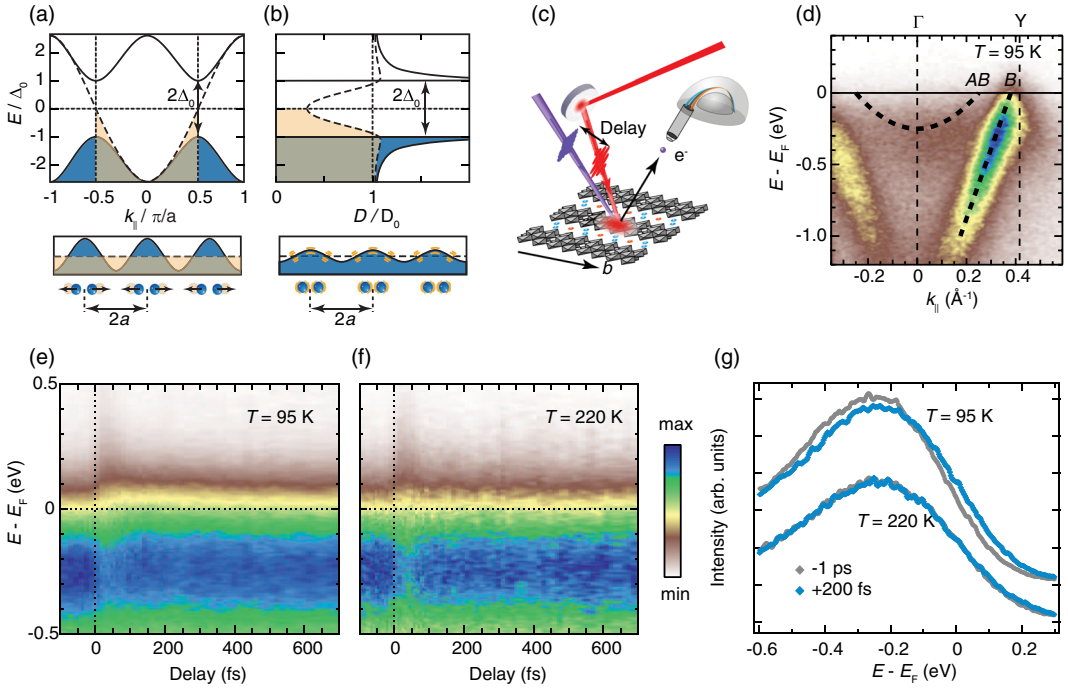

FIG. 1. (a),(b) Schematic illustration of (a) coherent lattice-vibration-induced closing of the CDW gap in the band structure $E(k_\parallel)$ and (b) incoherent lattice-fluctuation-induced filling-in of the gap in the density of states $D(E)$ (dashed lines, yellow shading). Solid lines and blue shading indicate the characteristic signatures of the canonical CDW state: the opening of the energy gap $2\Delta_0$, the modulation of the conduction electron density, and the associated periodic lattice distortion with lattice periodicity $2a$. (c) Sketch of the experimental setup and crystal structure of $Rb_{0.3}MoO_3$. (d) ARPES band map of the unpumped sample along the crystallographic b (Γ-Y) direction ($h\nu = 22.1$ eV, $T = 95$ K) revealing the dispersion of the bonding (B) and antibonding (AB) bands (dashed lines). (e),(f) Time-dependent ARPES spectra taken around the Fermi wave vector of the B band (e) at an equilibrium sample temperature of $T = 95$ K, i.e., below the CDW transition temperature, and (f) at an equilibrium sample temperature of $T = 220$ K, i.e., above the CDW transition temperature ($F = 0.59$ mJ cm^{-2}). (g) Energy distribution curves extracted from the data in (e) and (f) at selected pump-probe time delays.

structure calculations [41,42], the two relevant bands near the Fermi level (E_F) are resolved: the weakly intense and weakly dispersive antibonding (AB) band and the strongly intense and strongly dispersive bonding (B) band, which we will focus on in the following.

The photoinduced temporal evolution of the spectrum around the Fermi wave vector of the B band is shown in Figs. 1(e) and 1(f) for equilibrium sample temperatures below and above T_{CDW}, respectively. Upon excitation of the CDW state ($T < T_{CDW}$), the spectral weight peak associated with the B band is first suppressed in intensity and then shifts toward E_F. For the normal state ($T > T_{CDW}$), by contrast, no such peak shift is observed under otherwise identical measurement conditions. This distinct temperature-dependent spectrotemporal response is further corroborated by the comparison of energy distribution curves (EDCs) at selected pump-probe time delays shown in Fig. 1(g) (Supplemental Material, Fig. S1 [35]).

The time- and energy-dependent ARPES intensity difference map in Fig. 2(a) reveals how the spectral weight dynamics in the CDW state proceeds in characteristic energy windows above and around E_F. Figure 2(b) compares the corresponding transient ARPES intensity integrated over portions of these distinct intervals (Supplemental Material, Fig. S2 [35]).

Far above E_F and the gap (≈0.3–0.85 eV), the quasi-instantaneous rise ($\tau_{e,0} \approx 30$ fs, limited by the experimental time resolution) and rapid exponential decay (time constant of 30 ± 5 fs) of the spectral weight reflect the creation and relaxation of hot electrons at high energies, respectively. Directly above the gap edge (≈0.06–0.3 eV), the initial rise is still quasi-instantaneous, but the electron relaxation considerably slows down and shows a biexponential decay (time constants of 190 ± 20 and 2800 ± 300 fs). Figure 2(c) shows that this electron energy-dependent intensity relaxation is reflected in biexponential decay (time constants $\tau_{e,1} = 45 \pm 6$, $\tau_{e,2} = 580 \pm 150$ fs) of the transient total electron energy as approximated by the first moment of the spectral weight distribution above E_F, $E_t = \int_0^{0.85\,\mathrm{eV}} dE\, E\, I_B(E,t)$. The electron density, on the other hand, which is roughly proportional to the transient integrated spectral weight, $N_t = \int_0^{0.85\,\mathrm{eV}} dE\, I_B(E,t)$, displays single exponential decay (time constant of 330 ± 50 fs). The observed dynamics is characteristic for rapid, substantial hot-electron energy relaxation through emission of strongly coupled phonons, followed by slower electron-phonon

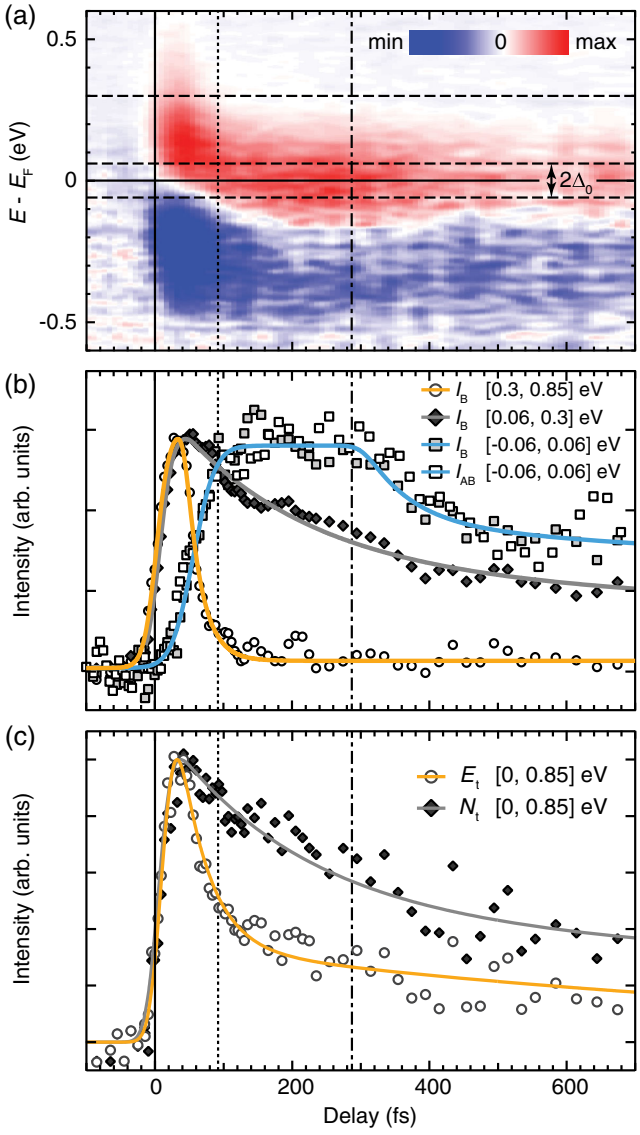

FIG. 2. (a) Energy-versus-time map of the photoinduced change of the ARPES intensity near the Fermi wave vector of the B band ($T = 95$ K, $F = 0.59$ mJ cm^{-2}). Dashed horizontal lines mark spectral regions with distinct dynamics, whereas the dotted and the dash-dotted vertical lines indicate the two characteristic timescales of the dynamics in the gap region. The filling-in of spectral weight in the gap ($|E - E_F| \leq 60$ meV) happens on a similar sub-100-fs timescale (dotted vertical line) as the relaxation of the photoinduced spectral weight at high energies ($E - E_F \geq 300$ meV), which is significantly faster than the timescale set by the structural bottleneck (dash-dotted vertical line). (b) Time and spectral region-dependent ARPES intensity near the Fermi wave vectors of the B and AB band with fits (solid lines). (c) Time-dependent zeroth (N_t) and first moment (E_t) of the B-band ARPES intensity distribution above the Fermi level with fits (solid lines). The quantities N_t and E_t are measures for the number and total energy of the hot electrons above E_F, respectively.

thermalization and recombination of low-energy electrons across the gap region, as known from experimental and theoretical studies of other material systems [43–46].

Remarkably, qualitatively different dynamics is detected in the CDW gap region (≈ -0.06–0.06 eV). The initial increase in intensity is prolonged to about 100 fs [sigmoidal time constant $\tau_\Delta = 60 \pm 10$ fs, dotted vertical line in Fig. 2(b)] and followed by a characteristic intensity plateau [14,21], which extends until about 280 fs after excitation [dash-dotted vertical line in Fig. 2(b)], before relaxation sets in (with an exponential time constant of 120 ± 40 fs). Such transient behavior is reminiscent of the typical two-step melting of CDW order in which a rapid electronic quench is superimposed on a slower damped coherent lattice relaxation [13–15,21] (Supplemental Material, Fig. S6 [35]). Indeed, the end time of the plateau corresponds to the typical structural bottleneck time, $\tau_A/2$, where τ_A is the oscillation period of the CDW amplitude mode ($\tau_A/2 \approx 315$ fs for $Rb_{0.3}MoO_3$ [47], Supplemental Material, Figs. S4 and S5 [35]). The intriguing observation, however, is that the filling-in of the gap is much faster and appears to be correlated, not with the photoinduced heating of the electrons, as expected for a purely electronic process, but with the initial fast electron energy relaxation [see solid orange, solid blue, and dotted vertical line in Fig. 2(b)]. In the Supplemental Material [35], this novel aspect to the generic two-timescale spectral response is brought out in a direct comparison with a layered CDW material (Supplemental Material, Fig. S6 [35]).

To further quantify and elucidate the gap dynamics, we plot in Fig. 3 the results of a line shape analysis in which the time-dependent quasiparticle peak at the lower gap edge was approximated with a Lorentzian on a constant background, multiplied by a Fermi-Dirac function and convoluted with a Gaussian representing the experimental energy resolution (Supplemental Material, Figs. S3 and S9 [35]). At the available experimental energy resolution (250 meV), the model can capture the dynamics of three characteristic spectral parameters—the broadening of the electron energy distribution ($k_B \Delta T_e$) and the shift (ΔE_{shift}) and broadening (ΔE_{broad}) of the quasiparticle peak—irrespective of the fact that the distribution function may be nonthermal and the spectral function non-Lorentzian [5,6,33] (Supplemental Material, Fig. S9 [35]). At a crude level, the three parameters may be regarded as measures for the excitation density of the electron gas (effective electron temperature), reduction of the energy gap, and quasiparticle scattering rate, respectively.

Figure 3(a) compares the extracted time dependencies of $k_B \Delta T_e$, ΔE_{shift}, and ΔE_{broad} for a dataset collected at an incident pump fluence of $F = 0.59$ mJ cm^{-2}. The transients of $k_B \Delta T_e$ and ΔE_{shift} reproduce the temporal evolutions of E_t, the total electron energy above E_F [Fig. 2(c)], and the spectral weight in the gap region [Fig. 2(b)], respectively. The quasi-instantaneous (~30 fs) increase of $k_B \Delta T_e$ to a value corresponding to about 1100 K is followed by a biexponential decay ($\tau_{e,1} = 40 \pm 5$, $\tau_{e,2} = 2300 \pm 150$ fs), once again indicative of a two-step

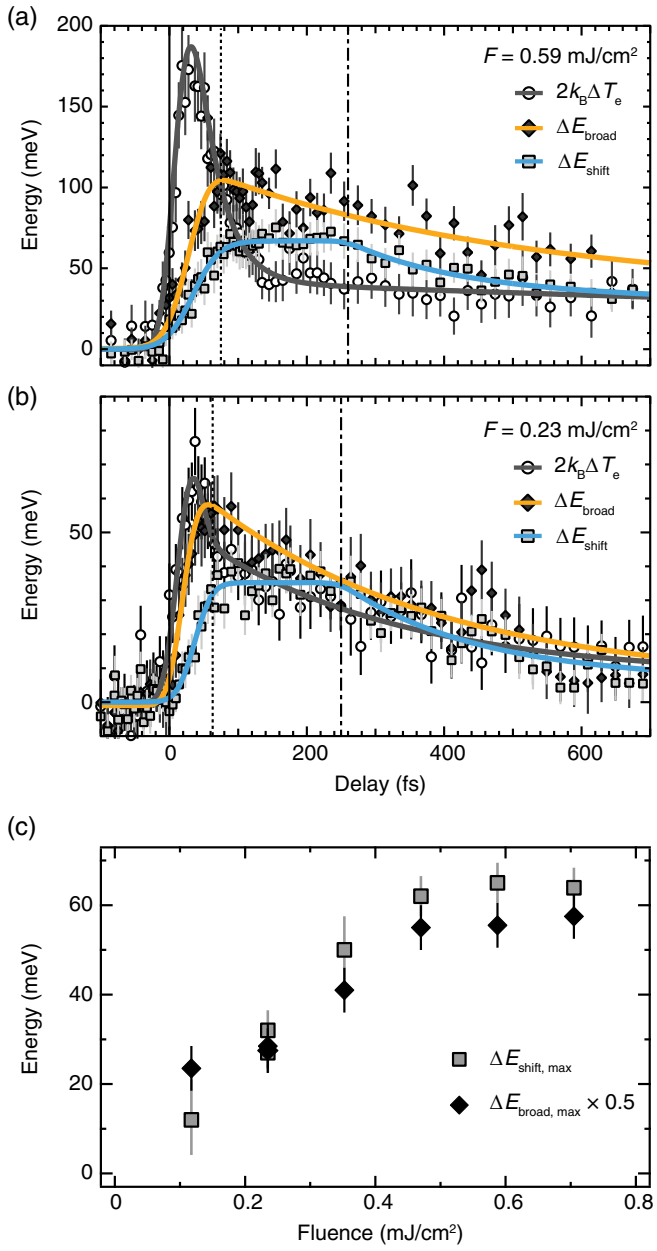

FIG. 3. (a),(b) Temporal evolution of the width of the leading edge ($k_B\Delta T_e$) and the broadening ($\Delta E_{\mathrm{broad}}$) and shift ($\Delta E_{\mathrm{shift}}$) of the spectral function peak, measured at $T = 95$ K and pump fluences of 0.59 (a) and 0.23 mJ cm^{-2} (b). Fits to the data are displayed as solid lines. The dotted and dash-dotted vertical lines indicate characteristic timescales of the transient spectral shift. The timescales for the initial spectral shift and broadening are similar (dotted vertical lines). The transient broadening shows similar rise rates and relaxation time constants (Supplemental Material, Fig. S7 [35]). (c) Maximum spectral shift and maximum spectral broadening as a function of pump fluence. Error bars represent standard uncertainties of the fitted parameters. Extra data points at 0.23 mJ cm^{-2} were recorded in a different experimental configuration.

relaxation process initially driven by the interaction with strongly coupled phonons. Remarkably, the fast relaxation component stops for both fluences at approximately the same value of $k_B\Delta T_e \approx 40$ meV, hinting at a closure of the fast relaxation channel at a characteristic threshold energy for phonon emission [48,49]. In contrast, the transient $\Delta E_{\mathrm{shift}}$ displays a slower rise to 65 meV with a sigmoidal time constant $\tau_\Delta = 60 \pm 10$ fs, stationary behavior between 100 and 280 fs, and then exponential decay (with a time constant of 220 ± 60 fs). We note that the transient peak broadening $\Delta E_{\mathrm{broad}}$ does not show plateaulike behavior, but exhibits a sigmoidal rise with a time constant identical to the one of the peak shift ($\tau_{\mathrm{broad}} = 60 \pm 18$ fs) as well as exponential decay (with a time constant of 480 ± 80 fs).

The correlation between the extracted spectral shift $\Delta E_{\mathrm{shift}}$ and broadening $\Delta E_{\mathrm{broad}}$ is also seen in the temporal evolution of the corresponding transients at a lower pump fluence [Fig. 3(b)], and in the fluence-dependent maximum shift and broadening [Fig. 3(c), Supplemental Material, Fig. S10 [35]]. The maximum $\Delta E_{\mathrm{shift}}$ and $\Delta E_{\mathrm{broad}}$ values both display saturation behavior at a critical incident fluence of about 0.6 mJ cm^{-2}. Notably, the saturation value of the peak shift is about 65 meV, consistent with the half-size of the equilibrium CDW gap (Δ_0) well below T_{CDW} [5], indicating that for excitation densities larger than the critical fluence the CDW gap is completely quenched [18]. The value of the saturation fluence is in rough agreement with the one reported previously for the complete suppression of the electronic component of CDW order [16].

The measured spectral weight and shape dynamics thus provide direct evidence for a photoinduced melting of the CDW gap that is, first, delayed with respect to hot carrier generation, but significantly faster than coherent lattice motion ($\tau_\Delta \ll \tau_A/2$) and, second, correlated with the initial fast relaxation of the electron energy (above the gap) in the presence of strong electron-phonon coupling and with an increase of the quasiparticle scattering rate (below the gap), as quantitatively manifested in the match of time constants: $\tau_\Delta \approx \tau_{e,1} \approx \tau_{\mathrm{broad}}$ (Supplemental Material, Table S1 [35]). This correlation between characteristic electronic processes around E_F, as directly measured by trARPES, is the central result of this work.

A natural explanation is that the suppression of the gap and concomitant increase of the quasiparticle scattering rate are driven by enhanced electron-phonon interactions, i.e., by the ultrafast, hot electron-induced generation of vibrational disorder. In contrast, the evident mismatch in the characteristic time constants $\tau_{e,0} < \tau_\Delta$, τ_{broad} and the transient (i.e., reversible) character of the gap quenching exclude dynamic electronic disorder and emerging static disorder due to photoinduced impurities as being the origin of the observed ultrafast melting of the CDW order, respectively. Lattice fluctuations [50] are indeed well

known to have a particularly strong effect on the electronic properties of quasi-one-dimensional CDW systems including the blue bronzes: They tend to give rise to a pseudogap with filled-in gap states and a smeared and shifted gap edge [31–33] [Fig. 1(b)], and they can cause strong electron scattering [2]. The ultrafast melting of the CDW gap in essence corresponds to the well-known suppression of the CDW peak due to phonon-induced disorder in ultrafast diffraction [12]. The remarkable aspects are the speed and dominance over the coherent CDW amplitude-mode vibration in the present case. Two types of phonon modes with strong-coupling behavior and vibrational periods short enough to be compatible with the observed fast disordering are likely to be important: high-frequency ($15\,\mathrm{THz} \leq f < 2\Delta_0/h \approx 29\,\mathrm{THz}$) "phase phonons" which are coupled to oscillations in the phase of the electronic order parameter of $Rb_{0.3}MoO_3$ [32,51,52], and the 28 THz (940 cm^{-1}) Mo-O stretching mode, which is sensitive to the CDW transition [53,54]. The elucidation of the specific underlying lattice dynamics, however, is beyond the capabilities of trARPES and calls for a direct probing of phonon couplings and populations by ultrafast diffuse scattering techniques [55]. We speculate that the rapid atomic disordering due to mode-selective emission of (high-frequency) CDW-coupled phonons by hot electrons, as uncovered here, may be a more generic phenomenon [12,56] than the recently demonstrated collective launch of incoherent phonons driven by an ultrafast change to a highly anisotropic, flat lattice potential [30].

Overall, the spectral weight dynamics revealed for $Rb_{0.3}MoO_3$ appears to be driven by strong electron-phonon coupling. This implies that, in the molybdenum blue bronzes, electron-phonon interactions [5] rather than electron-electron interactions [6] provide the dominant contribution to the spectral properties near E_F. More generally, in establishing a novel incoherent pathway for the ultrafast melting of electronic order, our trARPES results highlight the dominant role that lattice fluctuations can play in the sub-100-fs dynamics of low-dimensional quantum materials.

We thank Holger Fehske and Alexander Kemper for helpful discussions. This work was supported by the German Research Foundation (DFG) through project BA 2177/9-1 and the National Natural Science Foundation of China (Grant No. 11774190). L. X. Y. is grateful to the Alexander von Humboldt foundation for support.

*lxyang@tsinghua.edu.cn
†rossnagel@physik.uni-kiel.de

[1] S.-K. Chan and V. Heine, J. Phys. F **3**, 795 (1973).
[2] W. L. McMillan, Phys. Rev. B **16**, 643 (1977).
[3] K. Rossnagel, J. Phys. Condens. Matter **23**, 213001 (2011).
[4] J. D. Budai, J. Hong, M. E. Manley, E. D. Specht, C. W. Li, J. Z. Tischler, D. L. Abernathy, A. H. Said, B. M. Leu, L. A. Boatner, and R. J. McQueeney, Nature (London) **515**, 535 (2014).
[5] L. Perfetti, S. Mitrovic, G. Margaritondo, M. Grioni, L. Forró, L. Degiorgi, and H. Höchst, Phys. Rev. B **66**, 075107 (2002).
[6] D. Mou, R. M. Konik, A. M. Tsvelik, I. Zaliznyak, and X. Zhou, Phys. Rev. B **89**, 201116(R) (2014).
[7] J. Demsar and K. Biljaković, and D. Mihailovic, Phys. Rev. Lett. **83**, 800 (1999).
[8] F. Schmitt, P. S. Kirchmann, U. Bovensiepen, R. G. Moore, L. Rettig, M. Krenz, J.-H. Chu, N. Ru, L. Perfetti, D. H. Lu *et al.*, Science **321**, 1649 (2008).
[9] S. Hellmann, M. Beye, C. Sohrt, T. Rohwer, F. Sorgenfrei, H. Redlin, M. Kalläne, M. Marczynski-Bühlow, F. Hennies, M. Bauer, A. Föhlisch, L. Kipp, W. Wurth, and K. Rossnagel, Phys. Rev. Lett. **105**, 187401 (2010).
[10] T. Rohwer, S. Hellmann, M. Wiesenmayer, C. Sohrt, A. Stange, B. Slomski, A. Carr, Y. Liu, L. M. Avila, and M. Kalläne *et al.*, Nature (London) **471**, 490 (2011).
[11] A. Cavalleri, T. Dekorsy, H. H. W. Chong, J. C. Kieffer, and R. W. Schoenlein, Phys. Rev. B **70**, 161102(R) (2004).
[12] M. Eichberger, H. Schäfer, M. Krumova, M. Beyer, J. Demsar, H. Berger, G. Moriena, G. Sciaini, and R. J. D. Miller, Nature (London) **468**, 799 (2010).
[13] J. C. Petersen, S. Kaiser, N. Dean, A. Simoncig, H. Y. Liu, A. L. Cavalieri, C. Cacho, I. C. E. Turcu, E. Springate, F. Frassetto *et al.*, Phys. Rev. Lett. **107**, 177402 (2011).
[14] S. Hellmann, T. Rohwer, M. Kalläne, K. Hanff, C. Sohrt, A. Stange, A. Carr, M. M. Murnane, H. C. Kapteyn, L. Kipp *et al.*, Nat. Commun. **3**, 1069 (2012).
[15] L. Perfetti, P. A. Loukakos, M. Lisowski, U. Bovensiepen, H. Berger, S. Biermann, P. S. Cornaglia, A. Georges, and M. Wolf, Phys. Rev. Lett. **97**, 067402 (2006).
[16] A. Tomeljak and H. Schäfer, D. Städter, M. Beyer, K. Biljakovic, and J. Demsar, Phys. Rev. Lett. **102**, 066404 (2009).
[17] H. Schäfer, V. V. Kabanov, M. Beyer, K. Biljakovic, and J. Demsar, Phys. Rev. Lett. **105**, 066402 (2010).
[18] H. Y. Liu, I. Gierz, J. C. Petersen, S. Kaiser, A. Simoncig, A. L. Cavalieri, C. Cacho, I. C. E. Turcu, E. Springate, F. Frassetto *et al.*, Phys. Rev. B **88**, 045104 (2013).
[19] S. de Jong, R. Kukreja, C. Trabant, N. Pontius, C. F. Chang, T. Kachel, M. Beye, F. Sorgenfrei, C. H. Back, and B. Bräuer *et al.*, Nat. Mater. **12**, 882 (2013).
[20] H. Schaefer, V. V. Kabanov, and J. Demsar, Phys. Rev. B **89**, 045106 (2014).
[21] C. Sohrt, A. Stange, M. Bauer, and K. Rossnagel, Faraday Discuss. **171**, 243 (2014).
[22] T. Huber, S. O. Mariager, A. Ferrer, H. Schäfer, J. A. Johnson, S. Grübel, A. Lübcke, L. Huber, T. Kubacka, C. Dornes, C. Laulhe, S. Ravy, G. Ingold, P. Beaud, J. Demsar, and S. L. Johnson, Phys. Rev. Lett. **113**, 026401 (2014).
[23] M. Porer, U. Leierseder, and J. M. Ménard, H. Dachraoui, L. Mouchliadis, I. E. Perakis, U. Heinzmann, J. Demsar, K. Rossnagel, and R. Huber, Nat. Mater. **13**, 857 (2014).
[24] P. Beaud, A. Caviezel, S. O. Mariager, L. Rettig, G. Ingold, C. Dornes, S. W. Huang, J. A. Johnson, M. Radovic, T. Huber *et al.*, Nat. Mater. **13**, 923 (2014).
[25] V. R. Morrison, R. P. Chatelain, K. L. Tiwari, A. Hendaoui, and A. Bruhács, M. Chaker, and B. J. Siwick, Science **346**, 445 (2014).

[26] S. Mathias, S. Eich, J. Urbancic, S. Michael, A. V. Carr, S. Emmerich, A. Stange, T. Popmintchev, T. Rohwer, M. Wiesenmayer *et al.*, Nat. Commun. **7**, 12902 (2016).
[27] T. Frigge, B. Hafke, T. Witte, B. Krenzer, and C. Streubühr, A. Samad Syed, V. Mikšić Trontl, I. Avigo, P. Zhou *et al.*, Nature (London) **544**, 207 (2017).
[28] C. W. Nicholson, A. Lücke, W. G. Schmidt, M. Puppin, L. Rettig, R. Ernstorfer, and M. Wolf, Science **362**, 821 (2018).
[29] A. Zong, P. E. Dolgirev, A. Kogar, E. Ergeçen, M. B. Yilmaz, Y.-Q. Bie, T. Rohwer, I. Cheng Tung, J. Straquadine, X. Wang *et al.*, Phys. Rev. Lett. **123**, 097601 (2019).
[30] S. Wall, S. Yang, L. Vidas, M. Chollet, J. M. Glownia, M. Kozina, T. Katayama, T. Henighan, M. Jiang, T. A. Miller *et al.*, Science **362**, 572 (2018).
[31] R. H. McKenzie and J. W. Wilkins, Phys. Rev. Lett. **69**, 1085 (1992).
[32] L. Degiorgi, G. Grüner, K. Kim, R. H. McKenzie, and P. Wachter, Phys. Rev. B **49**, 14754 (1994).
[33] R. H. McKenzie, Phys. Rev. B **52**, 16428 (1995).
[34] S. Eich, A. Stange, A. V. Carr, J. Urbancic, T. Popmintchev, M. Wiesenmayer, K. Jansen, A. Ruffing, S. Jakobs, T. Rohwer *et al.*, J. Electron Spectrosc. Relat. Phenom. **195**, 231 (2014).
[35] See Supplemental Material at http://link.aps.org/supplemental/10.1103/PhysRevLett.125.266402 for details of (i) method, (ii) comparison of CDW- and normal-state trARPES results, (iii) spectral weight response below E_F, (iv) details about the fits to the data, (v) coherent oscillation of the CDW amplitude mode, (vi) simulation of the plateau in the spectral response, (vii) comparison of characteristic timescales for initial electronic and phononic short-time dynamics, (viii) spectral weight dynamics in comparison to a layered CDW compound, (ix) comparison of transient spectral broadening at low and high fluences, (x) transient spectral shift and broadening at long delays, (xi) Lorentzian versus Gaussian in the line shape analysis, and (xii) correlation between spectral weight shift and broadening, which includes Refs. [5,7,21,36–39].
[36] S. Ravy, H. Requardt, D. Le Bolloc'h, P. Foury-Leylekian, J.-P. Pouget, R. Currat, P. Monceau, and M. Krisch, Phys. Rev. B **69**, 115113 (2004).
[37] A. Tomeljak, B. Kavcic, and H. Schäfer, V. V. Kabanov, D. Mihailovic, D. Staresinic, K. Biljakovic, and J. Demsar, Physica (Amsterdam) **404B**, 548 (2009).
[38] A. D. Gromko, A. V. Fedorov, Y.-D. Chuang, J. D. Koralek, Y. Aiura, Y. Yamaguchi, K. Oka, Yoichi Ando, and D. S. Dessau, Phys. Rev. B **68**, 174520 (2003).
[39] J. D. Rameau, H.-B. Yang, G. D. Gu, and P. D. Johnson, Phys. Rev. B **80**, 184513 (2009).
[40] J. Wang, R. Xiong, F. Yi, D. Yin, M. Ke, C. Li, Z. Liu, and J. Shi, J. Solid State Chem. **178**, 1440 (2005).
[41] J.-L. Mozos, P. Ordejón, and E. Canadell, Phys. Rev. B **65**, 233105 (2002).
[42] B. Guster, M. Pruneda, P. Ordejón, E. Canadell, and J.-P. Pouget, Phys. Rev. Mater. **3**, 055001 (2019).
[43] V. V. Baranov and V. V. Kabanov, Phys. Rev. B **89**, 125102 (2014).
[44] T. Kampfrath, L. Perfetti, F. Schapper, C. Frischkorn, and M. Wolf, Phys. Rev. Lett. **95**, 187403 (2005).
[45] J. C. Johannsen, S. Ulstrup, F. Cilento, A. Crepaldi, M. Zacchigna, C. Cacho, I. C. Edmond Turcu, E. Springate, F. Fromm, C. Raidel, T. Seyller, F. Parmigiani, M. Grioni, and P. Hofmann, Phys. Rev. Lett. **111**, 027403 (2013).
[46] J. Tao, R. P. Prasankumar, E. E. M. Chia, A. J. Taylor, and J.-X. Zhu, Phys. Rev. B **85**, 144302 (2012).
[47] D. M. Sagar, D. Fausti, S. Yue, C. A. Kuntscher, S. van Smaalen, and P. H. M. van Loosdrecht, New J. Phys. **10**, 023043 (2008).
[48] D. Yadav, M. Trushin, and F. Pauly, Phys. Rev. B **99**, 155410 (2019).
[49] J. C. König-Otto, M. Mittendorff, T. Winzer, F. Kadi, E. Malic, A. Knorr, C. Berger, W. A. de Heer, A. Pashkin, H. Schneider, M. Helm, and S. Winnerl, Phys. Rev. Lett. **117**, 087401 (2016).
[50] S. Girault, A. H. Moudden, and J. P. Pouget, Phys. Rev. B **39**, 4430 (1989).
[51] M. J. Rice, Solid State Commun. **25**, 1083 (1978).
[52] M. D. Thomson, K. Rabia, F. Meng, M. Bykov, S. van Smaalen, and H. G. Roskos, Sci. Rep. **7**, 2039 (2017).
[53] R. Beyer, N. Barišić, and M. Dressel, Physica (Amsterdam) **407B**, 1823 (2012).
[54] R. Mankowsky, B. Liu, S. Rajasekaran, H. Y. Liu, D. Mou, X. J. Zhou, R. Merlin, M. Fórst, and A. Cavalleri, Phys. Rev. Lett. **118**, 116402 (2017).
[55] L. P. René de Cotret, J.-H. Pöhls, M. J. Stern, M. R. Otto, M. Sutton, and B. J. Siwick, Phys. Rev. B **100**, 214115 (2019).
[56] X. Shi, W. You, Y. Zhang, Z. Tao, P. M. Oppeneer, X. Wu, R. Thomale, K. Rossnagel, M. Bauer, H. Kapteyn, and M. Murnane, Sci. Adv. **5**, eaav4449 (2019).